

International Journal of Modern Physics E
© World Scientific Publishing Company

GROUND STATE PROPERTIES OF EVEN-EVEN AND ODD Nd, Ce AND Sm ISOTOPES IN HARTREE-FOCK-BOGOLIUBOV METHOD

Y. EL BASSEM[†] and M. OULNE*

*High Energy Physics and Astrophysics Laboratory, Department of Physics,
Faculty of Sciences SEMLALIA, Cadi Ayyad University,
P.O.B. 2390, Marrakesh, Morocco.*

[†]*younes.elbassem@edu.uca.ma*

**oulne@uca.ma*

Received Day Month Year
Revised Day Month Year

In this work, we have studied ground-state properties of both even-even and odd Nd isotopes within Hartree-Fock-Bogoliubov method with SLy5 Skyrme force in which the pairing strength has been generalized with a new proposed formula. We calculated binding energies, two-neutron separation energies, quadrupole deformation, charge, neutron and proton radii. Similar calculations have been carried out for Ce and Sm in order to verify the validity of our pairing strength formula. The results have been compared with available experimental data, the results of Hartree-Fock-Bogoliubov calculations based on the D1S Gogny effective nucleon-nucleon interaction and predictions of some nuclear models such as Finite Range Droplet Model (FRDM) and Relativistic Mean Field (RMF) theory.

Keywords: Hartree-Fock-Bogoliubov method; Nd , Sm and Ce isotopes; binding energy; proton, neutron and charge radii; two-neutron separation energies, quadrupole deformation.

PACS numbers: 21.10-k, 21.10.Dr, 21.10.Ft, 21.60-n

1. Introduction

In nuclear structure theory, several approaches have been developed to study ground-state and single-particle (s.p) excited states properties of even-even and odd nuclei. Among them we can find ab-initio calculations (Green's function - Monte Carlo shell model) based on bare N-N interaction for the lightest nuclei.¹ For medium-mass nuclei up to $A \sim 60$, the large-scale shell model² may be used. While for heavier nuclei, non-relativistic³⁻⁷ and relativistic^{8,9} mean field theories are mostly used. The most popular one among them is the Hartree-Fock method or the Hartree-Fock + BCS in which the pairing correlations are added to the mean

*corresponding author.

field via a corresponding potential term. Such methods give a good description of the nuclear structure near the line of β -stability.¹⁰ But, as one goes far from this line, the pairing correlations start to increase radically, so the HF+BCS theory ceases to be adequate for studying nuclei lying close to neutron and proton drip-lines. Thus, it is required to consider both the mean field and the pairing one self-consistently within the Hartree-Fock-Bogoliubov (HFB) Theory.¹¹

The aim of this work is to calculate and analyze some ground-state properties of even-even and odd Nd isotopes using Skyrme-Hartree-Fock-Bogoliubov method and a new generalized formula for the pairing strength for a wide range of neutron numbers. The ground-state properties we have focused on are binding energy, two-neutron separation energy, charge, proton and neutron radii. We have also performed similar calculations for Ce and Sm which are in the vicinity of Nd .

The paper is organized as follows: in Section II, we briefly describe the Hartree-Fock-bogoliubov method. In Section III, some details about the numerical calculations are presented while in Section IV, we present our results and discussion. A conclusion is given in Section V.

2. Hartree-Fock-Bogoliubov Method

In Hartree-Fock-Bogoliubov method, a two-body Hamiltonian of a system of fermions can be expressed in terms of a set of annihilation and creation operators (c, c^\dagger):

$$H = \sum_{n_1 n_2} e_{n_1 n_2} c_{n_1}^\dagger c_{n_2} + \frac{1}{4} \sum_{n_1 n_2 n_3 n_4} \bar{v}_{n_1 n_2 n_3 n_4} c_{n_1}^\dagger c_{n_2}^\dagger c_{n_4} c_{n_3} \quad (1)$$

with the first term corresponding to the kinetic energy and $\bar{v}_{n_1 n_2 n_3 n_4} = \langle n_1 n_2 | V | n_3 n_4 - n_4 n_3 \rangle$ are anti-symmetrized two-body interaction matrix-elements. So, the ground-state wave function $|\Phi\rangle$ is defined as the quasi-particle vacuum $\alpha_k |\Phi\rangle = 0$, in which the quasi-particle operators (α, α^\dagger) are connected to the original particle ones via a linear Bogoliubov transformation :

$$\alpha_k = \sum_n (U_{nk}^* c_n + V_{nk}^* c_n^\dagger), \quad \alpha_k^\dagger = \sum_n (V_{nk} c_n + U_{nk} c_n^\dagger), \quad (2)$$

In terms of the normal ρ and pairing κ one-body density matrices, defined as :

$$\rho_{nn'} = \langle \Phi | c_n^\dagger c_n | \Phi \rangle = (V^* V^T)_{nn'}, \quad \kappa_{nn'} = \langle \Phi | c_{n'} c_n | \Phi \rangle = (V^* U^T)_{nn'}, \quad (3)$$

the expectation value of the Hamiltonian (1) is expressed as an energy functional

$$E[\rho, \kappa] = \frac{\langle \Phi | H | \Phi \rangle}{\langle \Phi | \Phi \rangle} = \text{Tr}[(e + \frac{1}{2}\Gamma)\rho] - \frac{1}{2}\text{Tr}[\Delta\kappa^*] \quad (4)$$

where

$$\Gamma_{n_1 n_3} = \sum_{n_2 n_4} \bar{v}_{n_1 n_2 n_3 n_4} \rho_{n_4 n_2}, \quad \Delta_{n_1 n_2} = \frac{1}{2} \sum_{n_3 n_4} \bar{v}_{n_1 n_2 n_3 n_4} \kappa_{n_3 n_4}. \quad (5)$$

The variation of the energy (4) with respect to ρ and κ leads to the HFB equations:

$$\begin{pmatrix} e + \Gamma - \lambda & \Delta \\ -\Delta^* & -(e + \Gamma)^* + \lambda \end{pmatrix} \begin{pmatrix} U \\ V \end{pmatrix} = E \begin{pmatrix} U \\ V \end{pmatrix}, \quad (6)$$

where Δ and λ denote the pairing potential and Lagrange multiplier, introduced to fix the correct average particle number, respectively.

It should be stressed that the energy functional (4) contains terms that cannot be simply related to some prescribed effective interaction.¹² In terms of Skyrme forces, the HFB energy (4) has the form of local energy density functional:

$$E[\rho, \tilde{\rho}] = \int d^3\mathbf{r} \mathbf{H}(\mathbf{r}), \quad (7)$$

where

$$\mathbf{H}(\mathbf{r}) = H(\mathbf{r}) + \tilde{H}(\mathbf{r}) \quad (8)$$

is the sum of the mean field and pairing energy densities. The variation of the energy (7) according to the particle local density ρ and pairing local density $\tilde{\rho}$ results in Skyrme HFB equations:

$$\sum_{\sigma'} \begin{pmatrix} h(\mathbf{r}, \sigma, \sigma') & \tilde{h}(\mathbf{r}, \sigma, \sigma') \\ \tilde{h}(\mathbf{r}, \sigma, \sigma') & -h(\mathbf{r}, \sigma, \sigma') \end{pmatrix} \begin{pmatrix} U(E, \mathbf{r}\sigma') \\ V(E, \mathbf{r}\sigma') \end{pmatrix} = \begin{pmatrix} E + \lambda & 0 \\ 0 & E - \lambda \end{pmatrix} \begin{pmatrix} U(E, \mathbf{r}\sigma) \\ V(E, \mathbf{r}\sigma) \end{pmatrix}, \quad (9)$$

where λ is the chemical potential. The local fields $h(\mathbf{r}, \sigma, \sigma')$ and $\tilde{h}(\mathbf{r}, \sigma, \sigma')$ can be calculated in coordinate space. Details can be found in Refs. 13, 14, 15.

3. Details of Calculations

In the present study, a parametric form of total HFB energy with Skyrme force SLy5⁶ has been used as in Ref. 13. Ground state properties of even-even and odd ¹²⁴⁻¹⁶¹Nd have been reproduced by using the code HFBTHO (v2.00d)¹⁶ which utilizes the axial Transformed Harmonic Oscillator (THO) single-particle basis to expand quasi-particle wave functions. It iteratively diagonalizes the Hartree-Fock-Bogoliubov Hamiltonian based on generalized Skyrme-like energy densities and zero-range pairing interactions until a self-consistent solution is found.

Calculations were performed with the SLy5 Skyrme functional, a mixed surface-volume pairing with identical pairing strength for both protons and neutrons, and a quasi-particle cutoff of $E_{cut} = 60 \text{ Mev}$. The Harmonic Oscillator basis was characterized by the oscillator length $b_0 = -1.0$ which means that the code automatically sets b_0 by using $\hbar\omega_0 = 1.2 * 41/A^{1/3}$. The number of oscillator shells taken into account was $N_{max} = 16 \text{ shells}$, the total number of states in the basis $N_{states} = 500$, and the value of the deformation β is taken from the column β_2 of the Ref. 17. The number of Gauss-Laguerre and Gauss-Hermite quadrature points was $N_{GL} = N_{GH} = 40$, and the number of Gauss-Legendre points for the integration of the Coulomb potential was $N_{Leg} = 80$.

In the case of odd isotopes, calculations are made by using the blocking of quasi-particle states. The identification of the blocking candidate is done using the same technique as in HFODD¹⁸ : the mean-field Hamiltonian h is diagonalized at each iteration and provides a set of equivalent single-particle states. Based on the Nilsson quantum numbers of the requested blocked level provided in the input file, the code identifies the index of the quasi-particle (q.p.) to be blocked by looking at the overlap between the q.p. wave-function (both lower and upper component separately) and the s.p. wave-function. The maximum overlap specifies the index of the blocked q.p.¹⁶

There are different parameters sets of Skyrme forces for prediction of the nuclear ground-state properties.^{19,20} SLy5⁶ parameters set used in this study is given in Table 1.

Table 1. SLy5 parameters set.

Parameter	SLy5
t_0 (MeV fm ³)	-2484.88
t_1 (MeV fm ⁵)	462.18
t_2 (MeV fm ⁵)	-448.61
t_3 (MeV fm ⁴)	13673
x_0	0.825
x_1	-0.465
x_2	-1.0
x_3	1.355
W_0 (MeV fm ³)	126
σ	1/6

In the input data file of HFBTHO program (v2.00d),¹⁶ we have modified the values of the pairing strength for neutrons V_0^n and protons V_0^p (in MeV), which may be different, but in our study we have used the same pairing strength $V_0^{n,p}$ for both. At each time, we have executed the program and compared the obtained ground-state energy with the experimental value. This procedure was repeated until we found the value of $V_0^{n,p}$ that gives the ground-state energy closest to the experimental one.

The calculated ground-state energies of ^{124–161}Nd isotopes, obtained in this work with the corresponding pairing strength $V_0^{n,p}$, and the experimental data²¹ are listed in Table 2.

As can be noted from Table 2, there is a relationship between the pairing strength $V_0^{n,p}$ and the mass number A . By fitting the obtained values of $V_0^{n,p}$ to A , we have found the following formula :

$$\boxed{V_0^{n,p} = 170.95 A^{\frac{1}{6}}} \quad (10)$$

On Fig.1, we present two curves which show the variation of V_0 as a function of the mass number A . The solid curve is obtained from the data of Table 2, and the

Table 2. The ground-state energies of $^{124-161}\text{Nd}$ isotopes (in units of MeV) obtained in this work by using HFB method with SLy5 Skyrme force.

Nuclei	Experiment	Calcat	$V_0^{n,p}$	Nuclei	Experiment	Calcat	$V_0^{n,p}$
^{124}Nd	998.448	998.4436	380.9	^{143}Nd	1191.2596	1191.2528	393.1
^{125}Nd	1009.625	1009.6251	389.8	^{144}Nd	1199.0767	1199.0689	376.7
^{126}Nd	1022.994	1022.9924	381.8	^{145}Nd	1204.8319	1204.8252	392.9
^{127}Nd	1033.653	1033.6392	389.4	^{146}Nd	1212.3972	1212.3944	386.4
^{128}Nd	1046.528	1046.5205	384.0	^{147}Nd	1217.6894	1217.6898	392.9
^{129}Nd	1056.51	1056.5037	392.4	^{148}Nd	1225.0219	1225.0129	385.6
^{130}Nd	1068.9263	1068.9317	386.3	^{149}Nd	1230.0607	1230.0599	392.2
^{131}Nd	1078.1693	1078.1600	390.6	^{150}Nd	1237.4358	1237.4304	387.7
^{132}Nd	1089.8989	1089.8940	384.1	^{151}Nd	1242.7704	1242.7757	398.0
^{133}Nd	1098.8726	1098.8726	392.3	^{152}Nd	1250.048	1250.0499	392.9
^{134}Nd	1110.2623	1110.2661	382.0	^{153}Nd	1255.301	1255.3112	403.9
^{135}Nd	1118.9002	1118.9133	387.1	^{154}Nd	1261.722	1261.7247	396.1
^{136}Nd	1129.9573	1129.9546	380.8	^{155}Nd	1266.3965	1266.3885	405.4
^{137}Nd	1138.4138	1138.4186	388.2	^{156}Nd	1272.6636	1272.6725	398.8
^{138}Nd	1148.919	1148.9115	379.9	^{157}Nd	1276.7177	1276.7125	406.8
^{139}Nd	1156.9873	1156.9768	386.1	^{158}Nd	1282.328	1282.3388	399.1
^{140}Nd	1167.2976	1167.2870	370.4	^{159}Nd	1286.151	1286.1507	406.7
^{141}Nd	1175.3083	1175.3016	391.5	^{160}Nd	1291.68	1291.6796	400.3
^{142}Nd	1185.1361	1185.1350	377.7	^{161}Nd	1295.084	1295.0885	408.0

dashed one is the graphical representation of Eq. (10). The mean deviation between $V_{0_{fit}}$ and $V_{0_{exact}}$ is about 5.05 Mev.

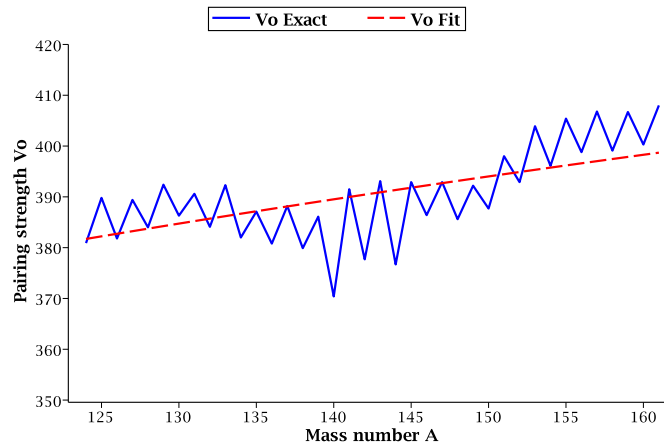


Fig. 1. The exact and adjusted pairing-strength $V_0^{n,p}$.

In order to verify the validity of Eq. (10), we have used this equation to generate the pairing-strength $V_0^{n,p}$ that we have included in the code HFBTHO (v2.00d) in order to calculate the ground-state properties for both even-even and odd $^{124-161}\text{Nd}$

isotopes. Also, the same calculations have been performed for $^{128-165}Sm$ and $^{119-157}Ce$ isotopes. The results are presented in the next section.

4. Results and Discussion

In this section we present the numerical results of this work, particularly for binding energy, two-neutron and two-proton separation energies and charge and neutron radii for $^{124-161}Nd$, $^{128-165}Sm$ and $^{119-157}Ce$ isotopes.

In all our calculations, we used the Skyrme (SLy5) force and Eq.(10) for the pairing strength.

4.1. Binding energy

In Fig.2, the calculated Binding Energy (BE) per nucleon for Nd isotopes, obtained by using the pairing strength generated by Eq. (10) as well as by direct calculations using the pre-defined pairing strength in HFBTHO(v2.00d) program¹⁶ are shown. Also, in Fig.2, we present the experimental binding energies per nucleon for Nd isotopes,²¹ the results of HFB calculations based on the D1S Gogny force²² and the obtained results in Ref. 23 in which the authors have used the code HFBTHO (v1.66p)¹³ to reproduce ground-state properties of even-even $^{142-164}Nd$ isotopes.

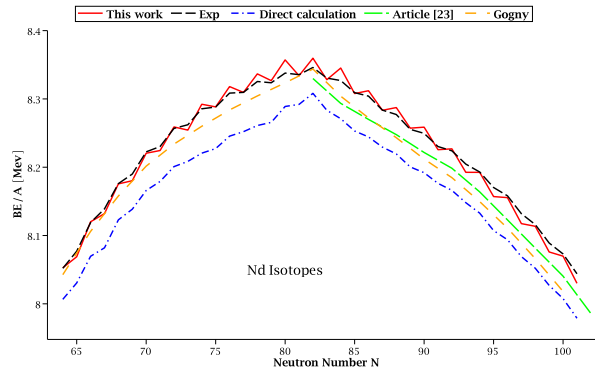


Fig. 2. Binding energies per nucleon for even-even and odd isotopic chains of Nd nuclei.

From Fig.2 we note that the maximum in the BE per nuclei is observed at the magic neutron number $N = 82$ in experimental data as well as in the HFB calculations based on the D1S Gogny force²² and HFB method with SLy5 Skyrme force for both direct calculations and calculations with Eq. (10). It should also be noted that using Eq. (10) gives improved results of the binding energy, and therefore, it will ameliorate the results of other ground-state properties of the nuclei.

The differences between the experimental BE per nucleon and the calculated results obtained in this work by using Eq. (10) are shown as function of the neutron

number N in Fig.3. The HFB calculations based on the D1S Gogny force²² as well as the predictions of Finite Range Droplet Model (FRDM)²⁴ and Relativistic Mean Field (RMF) model with NL3 functional⁹ are also included for comparison.

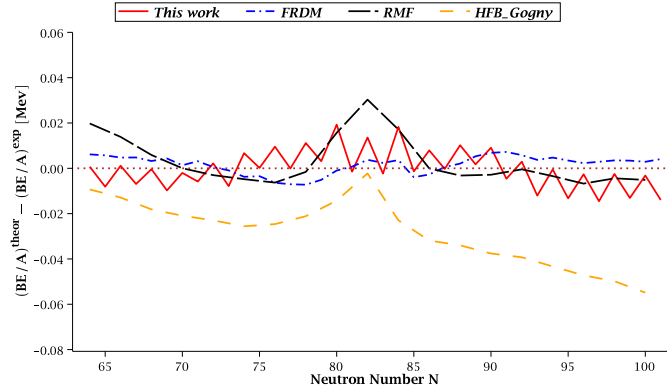


Fig. 3. The differences between our calculated results for binding energies per nucleon within HFB theory and experimental values,²¹ HFB calculations based on the D1S Gogny force²² and the predictions of both FRDM²⁴ and the RMF⁹ theories are shown for comparison.

As can be seen in Fig.3, the calculated BE per nucleon for Nd isotopes are in a good agreement with the experimental data. The maximal error is about 0.019 MeV per particle which corresponds approximately to 2.697 MeV for the total binding energy.

In order to ensure the validity of Eq. (10), we have used this equation to generate the pairing strength for neutrons and protons to calculate the ground state properties of two isotopic chains $^{119-157}Ce$ and $^{128-165}Sm$ which are in the vicinity of Nd . The differences between our calculated results for binding energies per nucleon within HFB theory and experimental values are displayed in Fig.4. The results of HFB calculations based on the D1S Gogny force²² as well as the predictions of the FRDM²⁴ and the RMF⁹ theories are displayed for comparison.

As can be seen in Fig.4, the calculated BE per nucleon for Ce and Sm isotopes in the HFB theory with SLy5 Skyrme force are in a good agreement with the experimental data in comparison with the other theoretical predictions. The approximately maximal errors per particle are 0.018 MeV and 0.020 MeV for Ce and Sm isotopes, respectively.

As a further verification of the validity of Eq. (10), we have used it to generate the pairing strength for the mass number $A = 140$ in order to calculate the total binding energy for even-even and odd isobars of ^{140}Nd , from $^{140}_{53}I_{91}$ to $^{140}_{69}Tm_{75}$. The calculated total binding energies and experimental data²¹ for this series of isobars are given as function of the proton number Z in Fig.5. The direct calculations as well as the HFB calculations based on the D1S Gogny force²² and the predictions

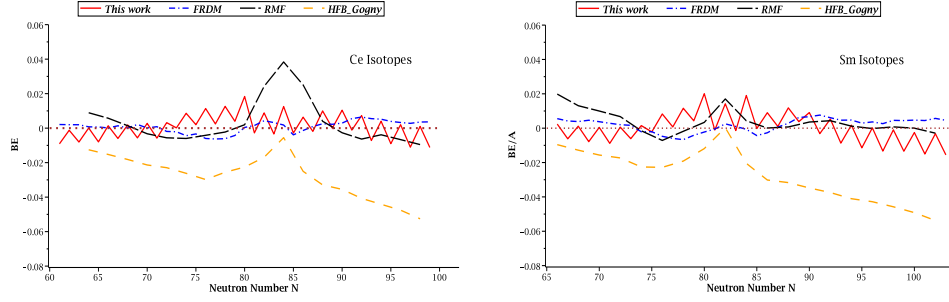


Fig. 4. Same as Fig.3, but for *Ce* isotopes (left) and *Sm* isotopes (right).

of both RMF⁹ and FRDM²⁴ theories are shown for comparison.

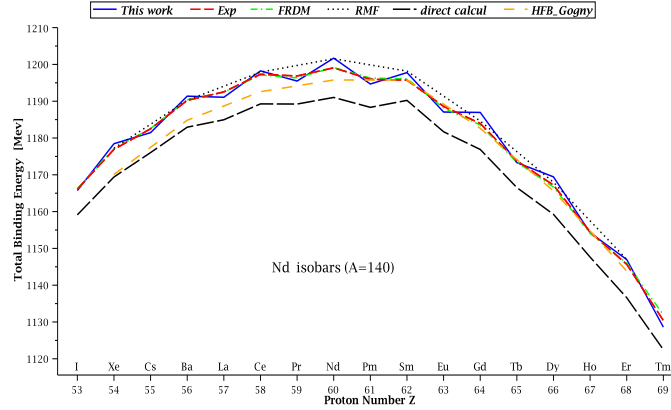


Fig. 5. The total binding energies of ¹⁴⁰Nd isobars

From Fig.5 we note that our calculated results for total binding energies of ¹⁴⁰Nd isobars are in a good agreement with those from experiment and FRDM and RMF theories. The use of Eq. (10) has improved the results of total binding energies compared to those of direct calculations. The mean absolute error between experimental data and results of this work is 1.436 Mev, while it is 0.347 Mev, 1.076 Mev, 3.123 and 7.392 Mev in FRDM,²⁴ RMF⁹ theory, HFB calculations based on the D1S Gogny force²² and direct calculations, respectively.

4.2. Neutron separation energy

The one-neutron and two-neutron separation energies are important quantities to exhibit the nuclear shell structure. In the present work, we calculated two-neutron separation energies (S_{2n}) for *Nd*, *Ce* and *Sm* isotopes in SLy5 parametrization with the pairing strength $V_0^{n,p}$ generated by Eq. (10).

The two-neutron separation energy is defined as

$$S_{2n}(Z, N) = BE(Z, N) - BE(Z, N - 2) \quad (11)$$

Note that when using this equation, all binding energies must be involved with a positive sign.

The calculated S_{2n} for Nd , Ce and Sm isotopes as well as experimental data,²¹ predictions of RMF⁹ and FRDM²⁴ theories, and HFB calculations based on the D1S Gogny force²² are presented in Fig.6.

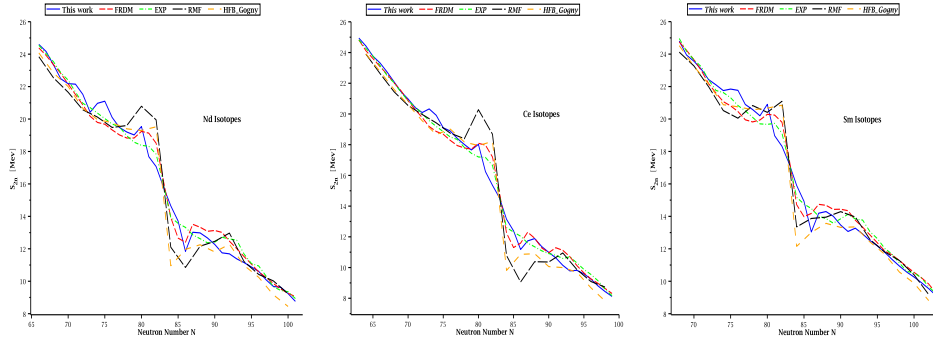


Fig. 6. Comparison of the calculated two-neutron separation energies S_{2n} of Nd , Ce and Sm isotopes with the RMF⁹ model, FRDM,²⁴ experimental data²¹ and HFB calculations based on the D1S Gogny force.²²

As can be seen in Fig.6, a sharp decrease in S_{2n} at the magic neutron number $N = 82$ corresponds to the closed shell. Also, the calculated two-neutron separation energies for Nd , Ce and Sm nuclei in HFB method with SLy5 Skyrme force as well as predictions of RMF theory with NL3 parameters set and FRDM theory are in a good agreement with experimental data. There are small differences between our results of HFB method with Skyrme force SLy5 and experimental data.

The approximately maximal errors of S_{2n} between the calculated results in the present study and experimental data for the three nuclei Nd , Ce and Sm are listed in Table 3. The predictions of FRDM and RMF theories as well as the HFB calculations based on the D1S Gogny force²² are listed too for comparison.

Table 3. The maximal difference error $(S_{2n})_{theor} - (S_{2n})_{exp}$ (in Mev).

Nuclei	This work	RMF	FRDM	HFB _{Gogny}
Nd	1.4782	2.4705	0.9205	2.98460
Ce	1.29951	3.07735	1.01289	2.78419
Sm	1.44676	1.96853	0.84682	3.02534

4.3. Neutron, Proton and Charge radii

The root-mean-square (rms) charge radius, R_c , is related to the proton radius, R_p , by

$$R_c^2 = R_p^2 + 0.64 \text{ (fm)} \quad (12)$$

In Fig.7 the root-mean-square charge radii predicted by our HFB calculations are compared with the available experimental data,²⁵ the predictions of RMF theory⁹ and the HFB calculations based on the D1S Gogny force.²²

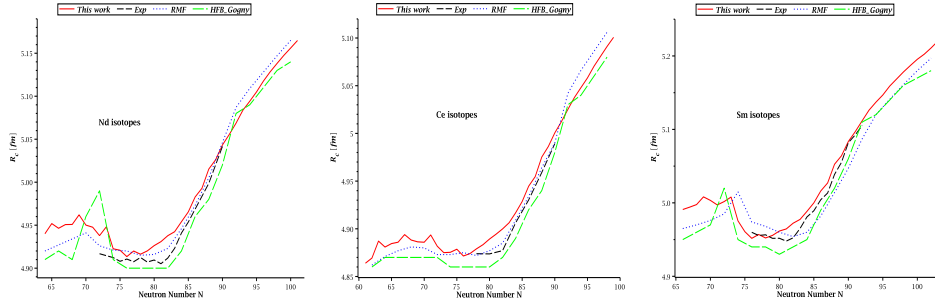


Fig. 7. The charge radii obtained by our HFB calculations compared with the available experimental data,²⁵ predictions of RMF theory⁹ and the HFB calculations based on the D1S Gogny force.²²

A good agreement between theory and experiment can be clearly seen in Fig.7. From this figure, one can see that the charge radii slightly decrease to the magic number when going from lighter to heavier isotopes. Therefore, the lighter isotopes have larger charge radii than the heavier closed-neutron-shell ($N=82$) nucleus. The charge radii of nuclei which are heavier than the closed-neutron-shell increase as well as the neutron number increases.

In order to better understand the structural evolution of *Nd* isotopes with increasing neutron number, the differences between squares of ground-state charge radii of *Nd* isotopes and those of the reference nucleus (The magic neutron number $N = 82$) have been calculated. The same calculations have been performed for $^{128-165}\text{Sm}$ and $^{119-157}\text{Ce}$ isotopes. The calculated and available experimental data²⁵ of $\langle r_N^2 \rangle - \langle r_{N=82}^2 \rangle$ are shown in Fig.8. The predictions of the RMF⁹ theory and the HFB calculations based on the D1S Gogny force²² are presented for comparison.

From Fig.8, it is seen a good agreement between the calculated results of $\langle r_N^2 \rangle - \langle r_{N=82}^2 \rangle$, the predictions of RMF⁹ theory, the HFB calculations based on the D1S Gogny force²² and the available experimental data.²⁵

Fig.9 shows the neutron and proton radii of *Nd*, *Ce* and *Sm* isotopes obtained in our calculations. The predictions of RMF theory and the HFB calculations based on the D1S Gogny force²² are also given for comparison. we have plotted neutron

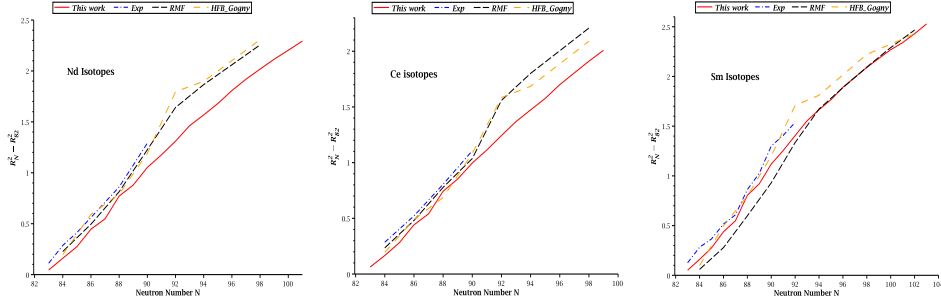


Fig. 8. The differences between squares of ground state charge radii : $\langle r_N^2 \rangle - \langle r_{N=82}^2 \rangle$ as function of neutron number.

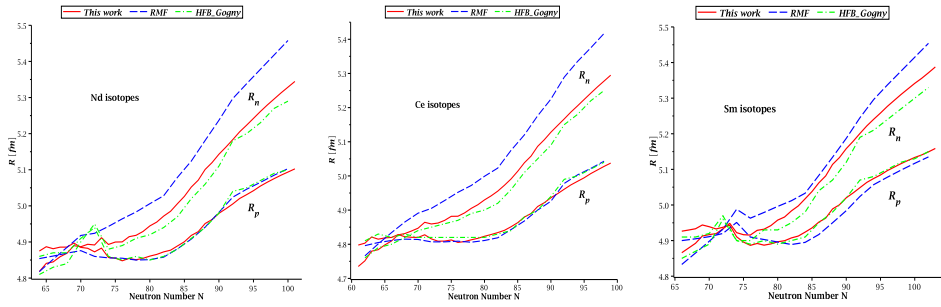


Fig. 9. The neutron and proton radii of *Nd*, *Ce* and *Sm* isotopes.

and proton radii (R_n and R_p) together in order to see the difference between them.

In the vicinity of the β -stability line ($N \approx Z$), the neutron and proton radii are nearly the same. But as the neutron number increases, the difference between the neutron and proton rms radii starts to increase in favour of developing a neutron skin. This difference reaches 0.242 fm for ^{161}Nd , 0.257 fm for ^{157}Ce and 0.228 fm for ^{165}Sm , which can be considered as an indication of possible neutron halo in *Nd*, *Ce* and *Sm* isotopes. On the other hand, the neutron radii of the three isotopic chains show a kink about the neutron shell closure ($N = 82$).

4.4. Quadrupole deformation

The deformations of nuclei play a crucial role in determining their properties such as quadrupole moment, nuclear sizes and isotope shifts. In this subsection we compare the quadrupole deformation parameters β_2 obtained by our calculations with available experimental data.²⁶ The β_2 values for the three isotopic chains considered in this work are shown in Fig.10. The results of the RMF²⁷ theory and the HFB calculations based on the D1S Gogny force²² are also presented for comparison.

As it can be seen from Fig.10, the agreement between different theoretical calculations, this work, HFB based on the D1S Gogny force²² and RMF²⁷ theory,

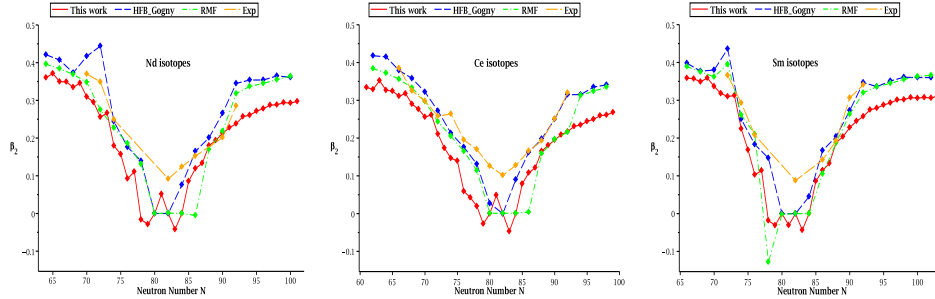


Fig. 10. The Quadrupole deformation Parameters β_2 for Nd, Ce and Sm isotopes.

and experimental data is quite good in general. The β_2 values show a minima at the magic neutron number $N = 82$ as expected, because almost all nuclei with $N = 82$ are spherical. Another well-known characteristic shown in Fig.10 is that the even-odd nucleus tends to be deformed despite that its neighboring even-even nuclei are spherical. The β_2 values obtained in this work as well as those of RMF²⁷ theory, HFB calculations based on the D1S Gogny force²² and available experimental data²⁶ manifest an interesting change of shapes of nuclei below and above the magic neutron number $N = 82$. For nuclei below $N = 82$, the three isotopic chains exhibit a transition from prolate shapes to spherical shapes, and for neutron number higher than $N = 82$, the prolate deformation increases and then saturates at a value which closes to $\beta_2 = 0.29$, $\beta_2 = 0.30$ and $\beta_2 = 0.26$ for Nd, Sm and Ce isotopes, respectively.

Here it should be noted that shape coexistence and shape mixing phenomena are not investigated in the present work, because we limited our calculations to the axial frame. To study these features, more sophisticated beyond-mean-field models are used, such as the Generator Coordinate Method (GCM),²⁸ and the Bohr Hamiltonian.²⁹

5. Conclusion

HFB theory with Skyrme force SLy5 has been employed to investigate the ground-state properties of even-even and odd *Nd*, *Ce* and *Sm* isotopic chains. Binding energies, two-neutron separation energies, quadrupole deformation and proton, neutron and charge radii for *Nd*, *Ce* and *Sm* isotopes have been calculated. These calculations have been performed by means of a new generalized formula for pairing strength $V_0^{n,p}$ for neutrons and protons. The use of this formula has improved the results of ground-state properties of the nuclei. The BE of *Nd*, *Ce* and *Sm* isotopes have been described successfully in this work. The parabolic behavior of the BE/A has been well reproduced in respect to the experimental curve. A possible neutron halo has been observed in the three series of isotopes *Nd*, *Ce* and *Sm*. The kink

related to isotopic shifts about the neutron-shell-closure ($N = 82$) was visible in our calculations, and the quadrupole deformation of Nd, Ce and Sm are well described with small differences from experimental results.

References

1. P. Navratil, B.R. Barrett and W.E. Ormand, Phys. Rev C56, 2542 (1997).
2. S. E. Koonin, D. J. Dean, and K. Langanke, Phys. Rep. 1, 278 (1997).
3. J. Dobaczewski, W. Nazarewicz, T.R. Werner, J.F.Berger, C.R. Chinn and J. Decharg, Phys. Rev. C 53, 2809 (1996).
4. J. Terasaki, P.-H. Heenen, H. Flocard and P. Bonche, Nucl. Phys. A600, 371 (1996).
5. M.V. Stoitsov, J. Dobaczewski, P. Ring and S. Pittel, Phys. Rev. C 61, 034311 (2000).
6. E. Chabanat, P. Bonche, P. Haensel, J. Meyer and R. Schaeffer, Nucl. Phys. A. 635, 231 (1998).
7. E. Terán, V.E. Oberacker, and A.S. Umar, Phys. Rev. C, 67, 064314 (2003).
8. P. Ring, Prog. Part. Nucl. Phys. 37, 193 (1996).
9. G. A. Lalazissis, S. Raman and P. Ring, *Atom. Data Nucl. Data Tables* 71, 1 (1999).
10. T.R. Werner, J.A. Sheikh, W. Nazarewicz, M.R. Strayer, A.S. Umar, and M. Misu, Phys. Lett. B 333, 303 (1994).
11. M. Yamagami, K. Matsuyanagi, and M. Matsuo, Nucl. Phys. A693, 579 (2001).
12. M. Bender, P. H. Heenen and P. G. Reinhard, Rev. Mod. Phys. 75, 121 (2003).
13. M. V. Stoitsov, J. Dobaczewski, W. Nazarewicz and P. Ring, Comp. Phys. Commun. 167, 43 (2005).
14. P. Ring and P. Schuck, *The Nuclear Many-Body Problem*, eds. W. Beiglbeck et al. (New York, Springer-Verlag, 1980).
15. W. Greiner, J. A. Maruhn, *Nuclear Models* Berlin, Springer-Verlag, (1995).
16. M. V. Stoitsov, N. Schunck, M. Kortelainen, N. Michel, H. Nam, E. Olsen, S. Wild, Comp. Phys. Commun. 184, 1592 (2013).
17. P. Moller, J. R. Nix, W. D. Myers, and W. J. Swiatecki. *Nuclear ground-state masses and deformations*. Atomic Data and Nuclear Data Tables, 59(2), 185-381, (1995).
18. J. Dobaczewski, W. Satua, B. G. Carlsson, J. Engel and al, Computer Physics Communications, 180(11), 2361-2391, (2009).
19. J. Bartel, P. Quentin, M. Brack, C. Guet and H. B. Hakkansson, Nucl. Phys. A. 386, 183 (1982).
20. A. Baran, J. L. Egido, B. Nerlo-Pomorska, K. Pomorski, P. Ring and L. M. Robledo, J. Phys. G. 21, 657 (1995).
21. M. Wang, G. Audi, A. H. Wapstra and al. -*The Ame2012 atomic mass evaluation*. Chinese Physics C, 36, 1603 (2012).
22. <http://www-phynu.cea.fr/HFB-Gognyeng.htm>.
23. S. O. Kara, T. Bayram, S. Akkoyun, Journal of Physics: Conference Series 490 012106, (2014).
24. P. Möller, J. R. Nix and K.-L. Kratz, *Atom. Data Nucl. Data Tables* 66, 131 (1997).
25. I. Angeli. *Atomic data and nuclear data tables*, 87(2), 185-206 (2004).
26. <https://www-nds.iaea.org/RIPL-2/masses/gs-deformations-exp.dat> (30/07/2015).
27. T. Bayram and A. H. Yilmaz, *Table of Ground State Properties of Nuclei in the RMF Model*. Modern Physics Letters A, 28(16), 1350068 (2013).
28. B. Bally, B. Avez, M. Bender, and P. H. Heenen, Physical review letters, 113(16), 162501, (2014).
29. M. Chabab, A. Lahbas and M. Oulne, Phys. Rev. C, 91, 064307 (2015).